Fracture Mechanics of Concrete and Concrete Structures - Assessment, Durability, Monitoring and Retrofitting of Concrete Structures- B. H. Oh, et al. (eds)
ⓒ 2010 Korea Concrete Institute, Seoul, ISBN 978-89-5708-181-5

Applicability of concrete using different admixtures to PC structures and their effects on improving durability

S. Yoshida
Civil Engineering Research Institute for Cold Region, Japan

T. Nawa
Hokkaido University, Japan

F. Taguchi
Civil Engineering Research Institute for Cold Region, Japan

H. Watanabe
Nittetsu Cement Co .Ltd, Japan

ABSTRACT: In this study, to improve the durability of concrete structures constructing newly or renewal, the physical properties and durability of concrete with binders combining high-early-strength Portland cement with different mineral admixtures were tested, and their applicability to prestressed concrete structures was examined. The results showed that their application to actual prestressed concrete structures was possible, although the strength development and drying shrinkage strain varied by the type of mineral admixtures used. The results of durability test also indicated that it was possible to improve the durability of concrete by selecting appropriate admixtures.

1 INTRODUCTION

There are a variety of methods for improving the durability of concrete structures against frost damage or deterioration caused by a combination of frost and salt damage. Such techniques include coating the concrete surface to prevent the infiltration of water, salt and other detrimental factors into the concrete or using epoxy-coated reinforcing bars to prevent the corrosion of steel inside concrete in cases where detrimental factors have already infiltrated. Meanwhile, improving the durability of concrete material by densification or other effects is the most fundamental measure, and it will be possible to reduce life-cycle costs efficiently if the long-term durability of concrete can be ensured.

From these backgrounds, the authors conducted a wide range of studies of the physical properties and durability of concrete using belite-based cement and ground granulated blast-furnace slag for the purpose of developing concrete with long-term durability. The results showed that highly pulverized belite-based cement or replacing part of it with ground granulated blast-furnace slag makes it possible to realize highly durable concrete with improved physical properties, such as strength/heat generation characteristics, frost resistance and chloride penetration resistance (Yoshida et al. 2001, 2002, 2004a, 2004b). Since low heat generation and long-term strength development can be expected in concrete using such binders in addition to long-term durability, the technique is considered extremely useful particularly for bridge piers, abutments, retaining walls and other relatively large structures. Meanwhile, initial strength development is important along with durability for Prestressed Concrete (hereinafter referred to as PC) structures, as they require prestressing at an early material age. It is therefore possible that initial strength may not be satisfied with the above-mentioned binders, although this depends on the required level of strength.

For the above reasons, the physical properties and durability of concrete using high-early-strength cement and various admixtures were examined in this study to enable the practical use of highly durable concrete that can be applied to PC structures.

2 OUTLINE OF THE EXPERIMENT

2.1 *Materials*

Table 1 lists the materials used. As base cement, high-early-strength portland cement, which is used commonly for PC, was used in consideration of strength development at an early age. As mineral

Table 1. Materials used.

Cement	High-early-strength Portland cement (HP) 4770*, density: 3.15 g/cm^3
Mineral admixtures	Ground granulated blast-furnace slag (BS) 6020*, density 2.89 g/cm^3 Fly ash Type I (FI) 5250*, density 2.40 g/cm^3 Fly ash Type II (FII) 3710*, density 2.11 g/cm^3 Silica fume (SF) 130000*, density 2.20 g/cm^3
Fine aggregate	Inland sand from Noboribetsu, density 2.70 g/cm^3, water absorption 1.50%
Coarse aggregate	Crushed stone from Shiraoi, maximum size=25mm, density 2.68 g/cm^3, water absorption 1.91%
High-range AE water-reducing agent	Polycarboxylic acid-based agent
Defoamer	Polyether base

* Specific surface area (cm^2/g)

admixtures, fly ash Types I and II, silica fume and ground granulated blast-furnace slag which satisfy their respective Japanese Industrial Standards (JIS) values were used. Ground granulated blast-furnace slag (hereinafter referred to as slag) with a 6,000-cm^2/g surface area was used in consideration of improving durability. To improve early strength development and autogeneous shrinkage, 4% of gypsum dihydrate – a level within the range of the JIS – was mixed as an SO_3 volume. Two types of high-performance AE water-reducing agent were used depending on the dispersibility of binders, and a defoamer was also used to adjust the air content.

2.2 *Concrete mix proportions*

Table 2 lists the mix proportions of concrete. The symbol indicates the combination of cement type, mineral admixture type and replacement ratio of mineral admixture. The water-binder ratio (W/B) was fixed at 40% in this study, since the ratio for general PC including the precast concrete production is around 35 to 45%. Mineral admixtures were added to replace a certain percentage of the cement. The replacement ratios of slag and fly ash were set at 60 and 20%, respectively, as the upper limits of the equivalent replacement ratios for blast-furnace slag cement and fly ash cement Type B in consideration of the influence on the strength development and durability of concrete. While the replacement ratio for silica fume is usually 5 to 15%, 10% was adopted for this study since this is the ratio commonly used both in Japan and in other countries (Japan Society of Civil Engineers, 1995). The target slump of the concrete was 8.0±2.5 cm, and the target air content was 4.5±1%.

2.3 *Experiment items*

The experiments conducted in this study are outlined below. After the specimens were made, they were left in a laboratory at 90% relative humidity for one day. After that, they were demolded and cured using different conditions depending on the test methods.

2.3.1 *Physical properties test*

For the test of physical properties, compressive strength and tensile strength tests were conducted at five material ages (1, 3, 7, 28 and 91 days) in accordance with JIS A 1108 and JIS A 1113. The specimens were cured in water at 20°C until each test age. Moreover, young's modulus was also measured with a compressometer in accordance with JIS A 1149.

2.3.2 *Shrinkage test*

A drying shrinkage test was conducted to study the shrinkage properties. Drying shrinkage strain was measured using a strain gauge embedded at the center of the specimen at the time of preparation. A 10 x 10 x 40 cm prismatic specimen was cured in water at

Table 2. Mix proportions.

Symbol	Cement type	Admixture type	Admixture replacement ratio	Water-Binder ratio (%)	Sand agg. ratio (%)	SP* type	SP* content (B×%)	Unit volume of concrete (kg/m^3)					
								Water	Binder		Fine agg.	Coarse agg.	Deformer (B×%)
									Cement	Ad.			
HP	HP	-	-	40	46	A	0.65	139	348	-	877	1022	0.0007
HFI(20)		FI	20			A	0.60	128	256	64	890	1041	0.0005
HFII(20)		FII	20			A	0.60	128	256	64	890	1041	0.0005
HSF(10)		SF	10			B	0.70	136	306	34	876	1025	0.0030
HBS(60)		BS	60			A	0.60	128	128	192	891	1042	0.0020

* SP: high-performance AE water-reducing agent (dispersibility: B > A)

20°C for seven days. It was then left in a room at a constant temperature (20 ± 2°C) and humidity (relative humidity: 60 ± 5%), and the drying shrinkage and mass changes of the specimen were measured.

2.3.3 *Durability tests*

For durability tests, chloride penetration resistance and freeze-thaw resistance tests were conducted. The chloride penetration resistance was evaluated based on the effective diffusion coefficients of chloride ions, which were found in accordance with the test method for effective diffusion coefficient of chloride ion in concrete by migration (JSCE-G571-2003) (Japan Society of Civil Engineers, 2004). Considering the influence of curing, a cylinder specimen measuring φ10 x 20 cm cured in water for 91 days was cut into disks of 5 cm in thickness.

The freeze-thaw test in accordance with Method A of JIS A 1148 was started at a material age of 28 days, and freeze-thaw resistance was evaluated based on the relative dynamic modulus of elasticity and mass changes with the progress of freeze-thaw cycles. Two types of test, one using fresh water and the other using a 3% NaCl solution, were conducted in this study.

The scaling test was conducted in accordance with ASTM C672. A dike about 25 mm wide and 20 mm high was placed along the perimeter of the top surface of a 22 x 22 x 10 cm prismatic specimen (cross section: 22 x 22 cm), and the surface of the specimen was covered with approximately 6 mm deep of a test solution. After the preparing, freezing and thawing effects were applied with daily cycles of -18°C for 16 hours and 23°C for 8 hours (the specimens were moved between rooms set at the respective temperatures) to measure the scaling volume. In consideration of on-site curing conditions, the specimens were moisture-cured in a 20°C environment for 7 days, followed by atmospheric curing in an environment with humidity of 60% and temperature of 20°C until the age of 28 days before being used for the test. A 3% NaCl solution was used as the test solution to simulate combined deterioration with salt damage.

3 EXPERIMENT RESULTS AND DISCUSSION

3.1 *Relationship between compressive strength and age*

Figure 1 shows the relationship between compressive strength and age. The compressive strength of HSF(10) using silica fume at a age of one day was the greatest, and exceeded that of plain HP which was made with high-early-strength cement only. The strength of HFI(20) and HFII(20) using fly ash was almost equivalent, with no difference according to variations in the quality of fly ash, and was approximately 7.0 N/mm^2 smaller than the strength of HP. The strength of HBS(60) using ground granulated blast-furnace slag was the smallest at 16.5 N/mm^2. Subsequently, the strength increased for all mix proportions with the progress of age. While the strength of HSP(10) was similar to that of HP until 28 days, the strength development of HSF(10) was greater than that of HP after the age of 28 days. The strength of HBS(60), whose strength development at an early material age was small, increased sharply with the progress of age, exceeded that of fly ash at 7 days, equaled those of HP and HSF(10) at 28 days, and exceeded that of HP –even though it was slightly smaller than that of HSF(10) –at 91 days. While the strength of high-quality HFI(20) exceeded that of HFII(20) at 3 days in the cases where fly ash was used, no difference in strength increase was observed between them thereafter, and their strength at 91 days was lower than those of other binders.

The above results indicate that strength development varied by the type of admixture used. However, the compressive strength of all mix proportions exceeded 40 N/mm^2 – the value commonly used as the standard design strength for PC structures at 28 days. Since the age at which the strength of 30 N/mm^2 or greater required for the pre-tension system was satisfied was one day for HSF(10) and HP and three days for HFI(20), HFII(20) and HBS(60), the application of these mix proportions to PC structures is considered feasible from the viewpoint of strength.

3.2 *Relationship between tensile strength and compressive strength*

Figure 2 shows the relationship between tensile strength and age. Tensile strength generally corresponded well with compressive strength, and the early tensile strength up to a age of seven days was high for HSF(10) and HP. While the strength of HBS(60) was the lowest, it increased afterwards and became almost the same as that of HSF(10) at seven days and later. In the cases where fly ash was used, no clear difference according to the quality of fly ash was observed.

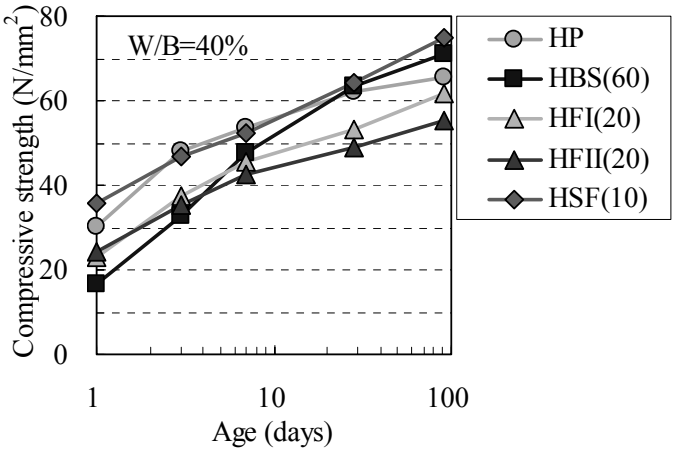

Figure 1. Relationship between compressive strength and age.

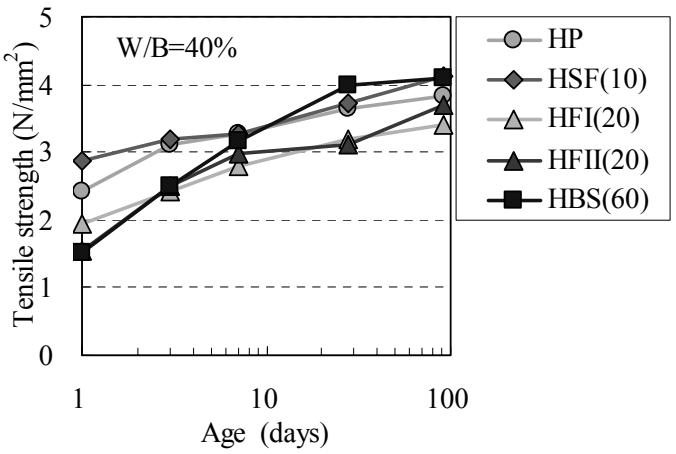

Figure 2. Relationship between tensile strength and age.

Figure 3 presents the relationship between tensile strength and compressive strength. It also shows the relationship between tensile strength and compressive strength calculated using an equation provided in the Japan Society of Civil Engineers (JSCE) Standard Specifications for Concrete Structures–2002 "Structural Performance Verification" (Japan Society of Civil Engineers, 2005a). While the figure indicates that tensile strength was slightly lower when fly ash was used, the relationship was almost the same as the calculated values from JSCE equation, and the correlation between tensile strength and compressive strength was high.

3.3 *Relationship between Young's modulus and compressive strength*

Figure 4 displays the relationship between Young's modulus and age. The Young's modulus of plain HP was high between 3 and 28 days, while those of HSF(10) using silica fume and the mixture using fly ash were almost uniform regardless of the age. While the value of HBS(60) using slag was small until a age of seven days, it increased dramatically thereafter as with the compressive strength, and reached its highest level at 91 days.

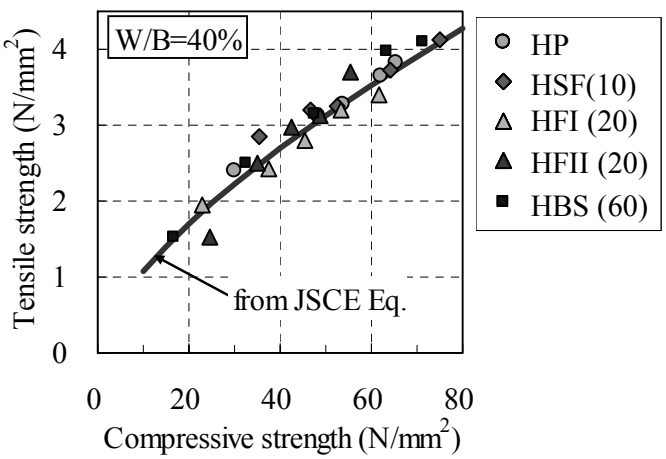

Figure 3. Relationship between tensile strength and compressive strength.

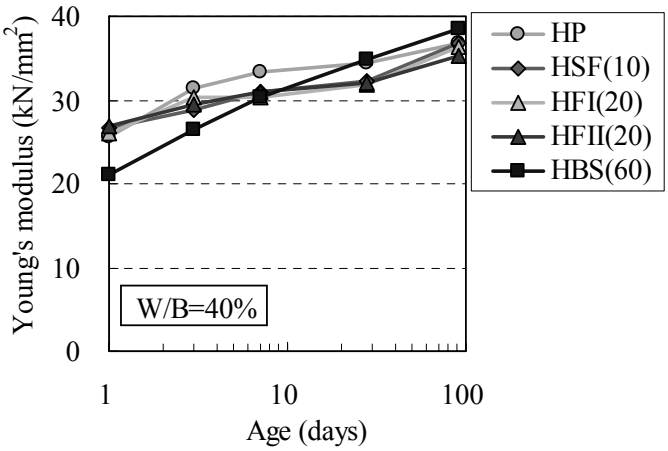

Figure 4. Relationship between young's modulus and age.

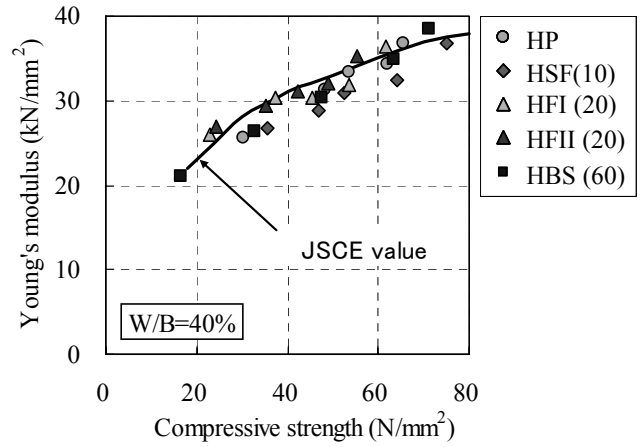

Figure 5. Relationship between Young's modulus and compressive strength.

Figure 5 shows the relationship between the Young's modulus and compressive strength. It also shows the relationship between the Young's modulus and compressive strength provided in the JSCE Standard Specifications for Concrete Structures–2002 "Structural Performance Verification" (Japan Society of Civil Engineers, 2005a). While the relationship between the static modulus of elasticity and compressive strength was generally good regardless of the type of binder, the modulus of elas-

ticity tended to be slightly lower than that shown in the specifications, although there were some exceptions.

3.4 *Properties of drying shrinkage*

Figure 6 shows the relationship between drying periods and drying shrinkage. Since drying shrinkage strain was not measured for HP and HFI(20) in this study, the figure also presents the drying shrinkage test results of concrete with commonly used ordinary portland cement (W/B = 40%, unit water volume = 138 kg/m^3, hereinafter referred to as ordinary cement) and blast-furnace slag cement Type B (W/B = 40%, unit water volume = 136 kg/m^3, hereinafter referred to as slag cement) as a reference. Refer to past studies for the mix proportions of these concrete (Yoshida et al, 2006). While the JSCE Standard Specifications for Concrete Structures–2002 "Materials and Construction" (Japan Society of Civil Engineers, 2005c) provides that the limit value of drying shrinkage strain can be generally set at around 500 to 700 μ, the measured values for ordinary cement and slag cement in the figure are slightly larger.

It can be seen that, while the shrinkage strain of HSF(10) using silica fume was higher than that of ordinary cement until a drying periods of around 50 days. However the relationship between the two reversed thereafter and the strain of HSF(10) became similar to that of HFII(20) using fly ash Type II. The shrinkage strain of HBS(60) using ground granulated blast-furnace slag was the lowest at all drying periods. While past studies have reported that the drying shrinkage in the early stages of drying (up to three weeks) tends to increase slightly when the specific surface area and replacement ratio of slag are greater (Japan Society of Civil Engineers, 1996), no such tendency was observed within the range of this study. The drying shrinkage of concrete with mineral admixtures was lower than those of commonly used ordinary cement and slag cement, regardless of the mineral admixture type in this study.

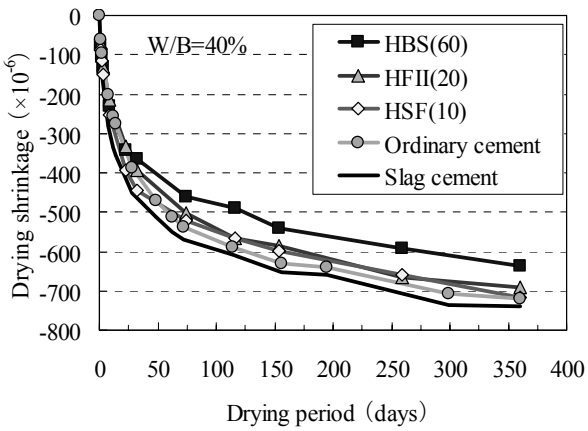

Figure 6. Relationship between drying periods and drying shrinkage.

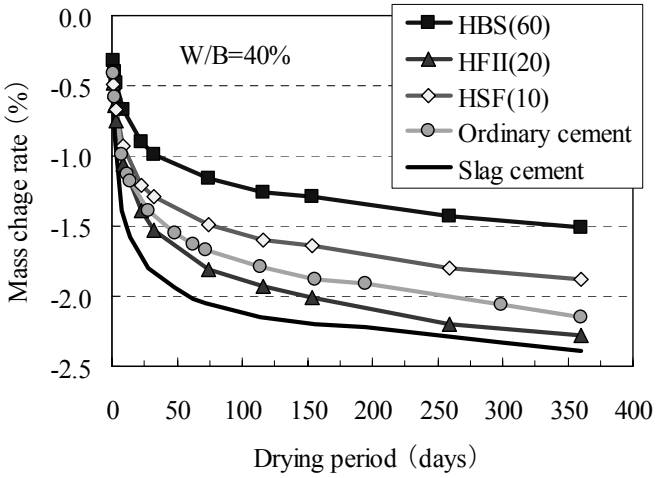

Figure 7. Relationship between drying periods and mass change rate.

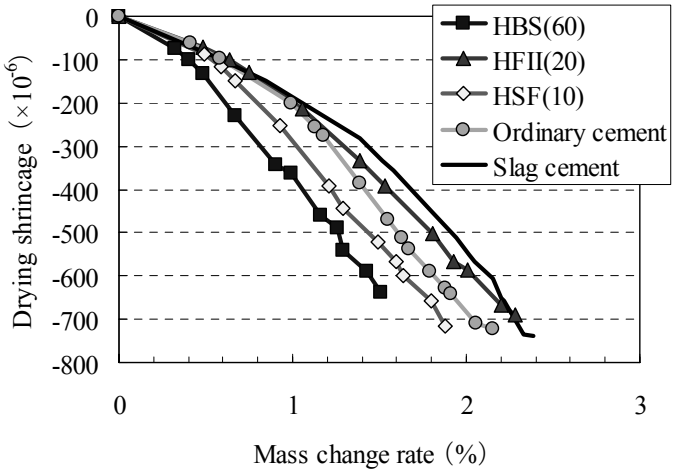

Figure 8. Relationship between mass change rate and drying shrinkage.

Figure 7 shows the relationship between the drying periods and mass change rate of the specimens. Mass change rate of HBS(60) for which the shrinkage strain was the lowest was also the lowest, followed by HSF(10) and HFII(20), and the mass change rate varied by the type of binder.

Figure 8 shows the relationship between the mass loss rate and drying shrinkage strain. The shrinkage strain generally increased with a higher mass loss rate, which was the lowest for HBS(60) with low shrinkage. Conversely, the shrinkage at a uniform mass change rate was the largest for HBS(60), followed by HSF(10) and HFI(20). The drying shrinkage mechanism cannot be explained arbitrarily, as opinions on the matter differ. However, according to the relatively common theory of capillary tension (E.g., Japan Concrete Institute, 1996), capillary tension generated when water in pores evaporates as a result of drying increases with smaller pore diameters. It is therefore presumed that shrinkage strain will increase in concrete with dense pores. However, since water in pores becomes difficult to evaporate and strength increases when pores are denser, the final shrinkage strain should be determined by considering not only the capillary tension depending on the

pore diameter size but also the total volume of evaporating water and strength.

In this study, considering the above mechanism, it was presumed that drying shrinkage of concrete with ground granulated blast-furnace slag decreased because the pore structure of concrete with slag became dense and the water in the pores became difficult to evaporate even though the shrinkage at a uniform mass loss rate was larger. As shown in Figure 1, the compressive strength after seven days when drying shrinkage test started was the highest for HSF(10), followed by HBS(60) and HFII(20), and the rate of increase in strength of HBS(60) was the highest. From the results means that the pore structure of HBS(60) is dense. The compressive strength shown in Figure 1 was measured after curing in water, and was different from the strength developed in concrete dried in a room at 20°C with a relative humidity of 60% at and after seven days. However, it has been reported that the strength of concrete using slag increases for around 100 days and its pore structure densifies through long-term hydration reaction after curing in water for seven days and drying in a room with a temperature of 20°C and a relative humidity of 50% (Japan Society of Civil Engineers, 1996). It was presumed that a similar phenomenon occurred in this study.

The above results indicated that, while the drying shrinkage strain increases with the mass loss of the specimens, the degree of shrinkage varies by the type of binder used. It is also considered that, regardless of the type of admixture used, drying shrinkage of concrete with admixtures is similar to or lower than that of concrete with ordinary cement, and is therefore applicable to actual structures. However, since these tendencies are thought to vary by the unit water volume of concrete as well as the age at which drying starts and the environmental conditions of application, it is considered important to select appropriate types of admixture based on mix and use conditions.

3.5 *Chloride penetration resistance*

Figure 9 displays the effective diffusion coefficient of chloride ion of concrete by migration test using electrophoresis. The figure also shows the test results of commonly used ordinary cement and slag cement. It can be seen that the effective diffusion coefficient of chloride ion of concrete with mineral admixtures was lower than that of HP, which was high-early-strength cement. The effective diffusion coefficients of HBS(60) and HSF(10) using ground granulated blast-furnace slag and silica fume were even lower than that of slag cement, which is commonly known to excel in chloride penetration resistance. However, the effective diffusion coefficient of concrete with fly ash were on a level similar to that of concrete with ordinary portland cement even though they were lower than that of concrete with high-early-strength cement, and the expected effect could not be achieved in this test.

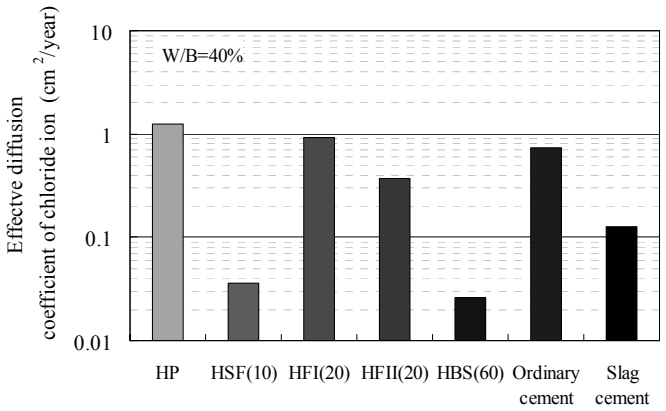

Figure 9. Effective diffusion coefficient of chloride ion.

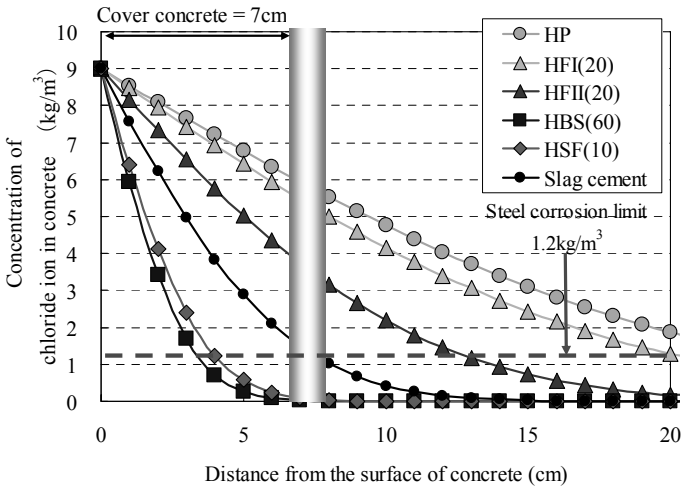

Figure 10. Prediction of chloride ion penetration after 100 years.

Figure 10 presents the results of predicting chloride ion penetration after 100 years, which was calculated using the effective diffusion coefficient and Fick's diffusion equation. The surface chloride ion content used for the prediction was 9.0 kg/m^3, which is equivalent to the value near the shoreline presented in the verification for chloride ions in the JSCE Standard Specifications for Concrete Structures–2002 "Materials and Construction" (Japan Society of Civil Engineers, 2005b). The figure indicates that sufficient resistance can be achieved with a standard cover depth of 7 cm in the cases of HBS(60) and HSF(10) and that contribution to a reduction of life-cycle costs is highly possible, while a cover depth of around 13 cm is necessary for HFII(20) to maintain the chloride content of concrete below the steel corrosion limit at the position of the steel reinforcement after 100 years. The effective diffusion coefficient is a figure that presents the degree of electrophoresis of chloride ions, unlike the apparent diffusion coefficient of chloride ion com-

monly used for salt-resistant design. Since the apparent diffusion coefficient may be included the effect of fixed and adsorption of chloride ion, it seems that the apparent diffusion coefficient is smaller than the effective diffusion coefficient. It is therefore seems to be possible to predict on the safe side by using the effective diffusion coefficient.

3.6 *Freeze-thaw resistance*

Figure 11 presents the results of freeze-thaw tests in fresh and salt water. In fresh water, changes in the relative dynamic modulus of elasticity and mass changes of HBF(60) using slag were the smallest, and the durability of HBF(60) improved more than that of HP. Although the relative dynamic modulus of elasticity of concrete with the other admixtures was slightly lower than that of HP, the relative dynamic modulus of elasticity after the completion of 300 freeze-thaw cycles was 85% or higher regardless of the type of binder, indicating extremely high frost resistance.

While deterioration was generally more serious in the tests using 3% NaCl solution compared with those using fresh water, both the relative dynamic modulus of elasticity and the mass loss rate of specimens with slag were on the same level as those in the cases using fresh water, indicating an extremely high resistance for these specimens. The values for plain HP and HSF(10) using silica fume remained on the same level. The relative dynamic modulus of elasticity was below 80%, and the mass loss rate increased to 10% or higher. For the specimens using fly ash Type I, the relative dynamic modulus of elasticity dropped to 70% and the mass loss rate reached its maximum of 20% after 300 cycles.

As outlined above, frost resistance varied by the characteristics of the test water. While resistance was always high in tests using fresh water, it varied by the type of binder in tests using salt water, indicating the necessity of selecting a binder appropriate for the environment. Since chloride penetration performance is also expected to decrease with reduced frost resistance, it is necessary to evaluate taking combined deterioration by frost and salt damage into account. However, when slag is used (as in this study), it is considered possible to control chloride penetration because frost deterioration is rather insignificant even in freeze-thaw tests using salt water. The feasibility of improving the durability of concrete in severe environments is therefore thought to be high.

3.7 *Scaling resistance*

Figure 12 shows the relationship between the scaling volume and the number of freeze-thaw cycles. The

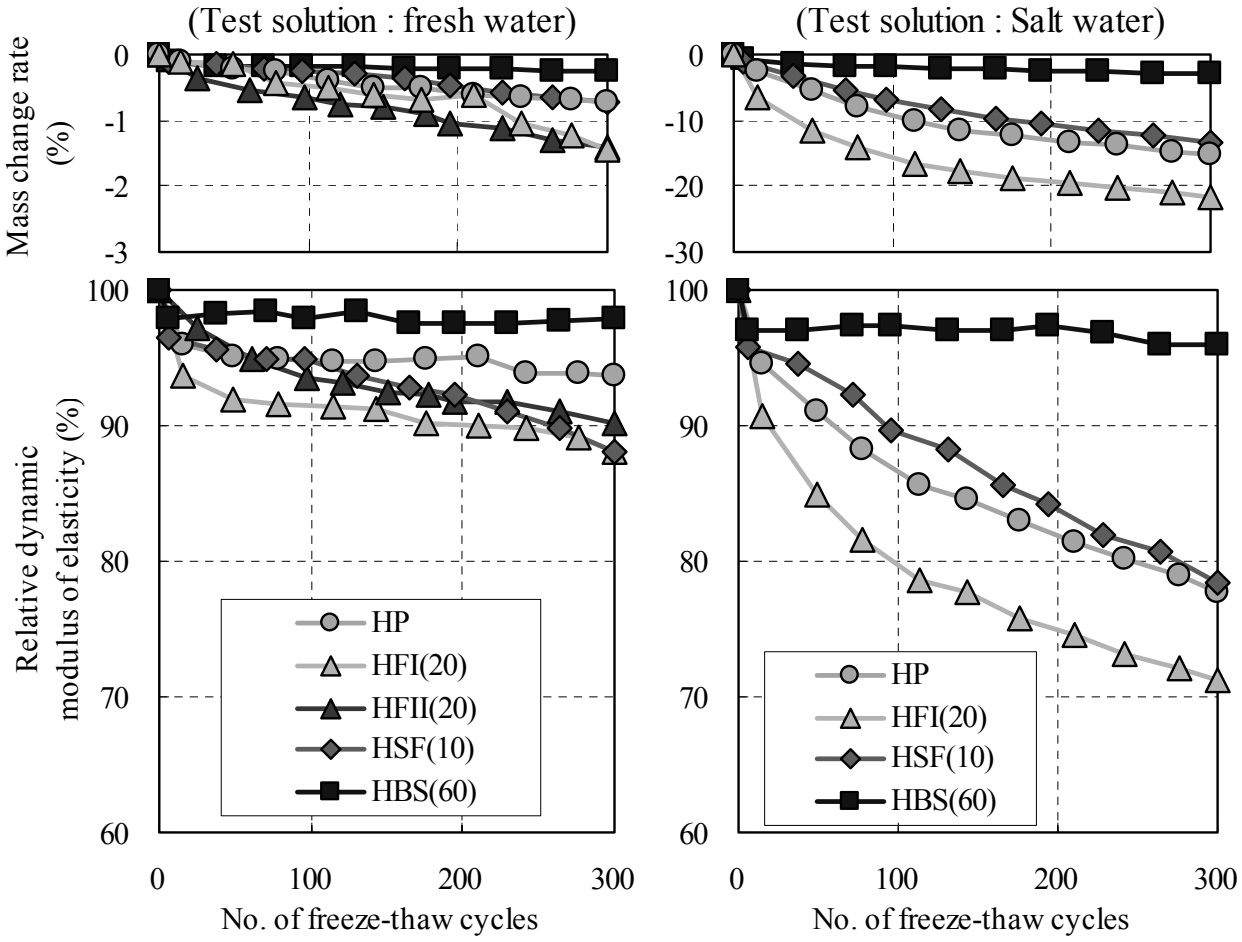

Figure 11. Results of Freeze-thaw test in water.

scaling volume of concrete with plain high-early-strength cement and fly ash Type I tended to be greater than those of concrete with other binders. Looking at the cases using other binders after the completion of 300 cycles, on the other hand, the scaling volume tended to increase at and after 75 cycles in the case of silica fume. The scaling volume of the specimen using slag was small, although it increased gradually. Scaling was controlled significantly in the specimen using fly ash Type II. It was thus found that the scaling volume tended to vary by the type of binder. These tendencies were similar to those in the results of the freeze-thaw test using 3% NaCl as shown in Figure 11. However, since the curing conditions and ages at which the tests were started were different between these tests, and the elution of $CaCl_2$ is possible when using salt water, it will be necessary in the future to conduct detailed studies on the effects of the pore structure and the $Ca(OH)_2$ content of concrete on durability.

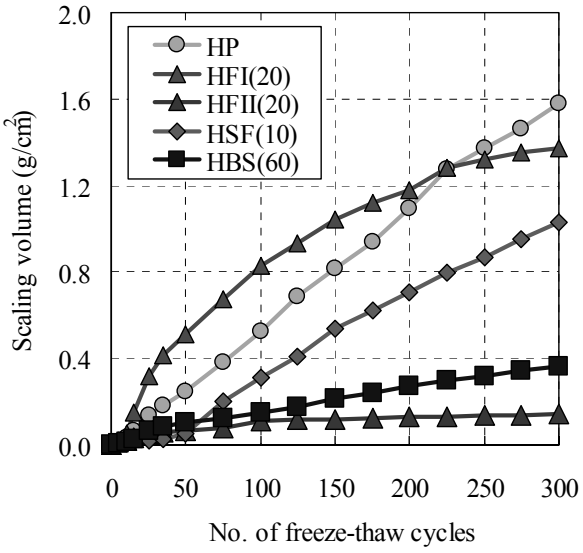

Figure 12. Relationship between scaling volume and freeze-thaw cycles.

4 CONCLUSIONS

In this study, the applicability of concrete using high-early-strength cement and different types of mineral admixture for PC structures was examined as a measure to improve durability of concrete structures. The main results of this study are that the application of concrete with these binders to actual prestressed concrete structures was possible, although the strength development and drying shrinkage strain varied by the type of mineral admixtures used and that it was possible to improve the durability of concrete by selecting appropriate admixtures.

REFERENCES

E.g., Japan Concrete Institute. 1996. Report of the Committee on Autogenous Shrinkage of Concrete: 51 – 54.

Japan Society of Civil Engineers. 1995. Recommendations for design and construction of concrete structures using silica fume in concrete -draft-, Concrete Library, No. 80: 5 – 9.

Japan Society of Civil Engineers. 1996. Recommendations for construction of concrete structures using ground granulated blast-furnace slag in concrete, Concrete Library, No. 86: 95 – 98.

Japan Society of Civil Engineers. 2004. JSCE Standards on test method for diffusion coefficient of chloride ion in Concrete, JSCE Guidelines for Concrete, No.2: 1 – 12.

Japan Society of Civil Engineers. 2005a. Standard Specifications for Concrete Structures – 2002 ”Structural Performance Verification”, JSCE Guidelines for Concrete, No.3: 24 – 32.

Japan Society of Civil Engineers. 2005b. Standard Specifications for Concrete Structures – 2002 “Materials and Construction”, JSCE Guidelines for Concrete, No.6: 30 – 34.

Japan Society of Civil Engineers. 2005c. Standard Specifications for Concrete Structures – 2002 “Materials and Construction”, JSCE Guidelines for Concrete, No.6: 66.

Yoshida, S., Taguchi, F. & Shimada, H. 2001. Strength, heat generation and freeze-thaw resistance of concrete using modified belite-based cement, Monthly Report of the Civil Engineering Research Institute of Hokkaido, No. 578: 4 – 13.

Yoshida, S., Taguchi, F. & Watanabe, H. 2002. Chloride permeability of modified belite-based cement concrete with blast-furnace slag, Proceedings of Japan Concrete Institute, Vol. 24, No. 1: 639 – 644.

Yoshida, S., Taguchi, F., Nawa, T. & Watanabe, H. 2004a. Study on chloride permeability of modified belite-based cement concrete with blast-furnace slag, Proceedings of Japan Concrete Institute, Vol. 26, No. 1: 777 – 782.

Yoshida, S., Taguchi, F., Nawa, T. & Watanabe, H. 2004b. Carbonation of modified belite-based cement concrete with blast-furnace slag, Proceeding of Hokkaido Chapter of the Japan Society of Civil Engineers, No. 60, Vol. 28: 766 – 767.

Yoshida, S., Taguchi, F., Nawa, T. & Watanabe, H. 2006. Scaling resistance of concrete mixed with various binders, The Proceedings of the 61st JSCE Annual Meeting, Vol. 391: 779 – 780.